RSC Advances

ROYAL SOCIETY OF CHEMISTRY

www.rsc.org/advances

Cite this: DOI: 10.1039/c0xx00000x

www.rsc.org/xxxxxx

PAPER

Synthesis and Properties of Single Crystal $TbMn_2O_5$ Nanostructures

Peikai Zhang, Yimin Cui*

Received (in XXX, XXX) Xth XXXXXXXXX 20XX, Accepted Xth XXXXXXXXX 20XX
DOI: 10.1039/b000000x

Single crystal nanowire clusters of multiferroic material $TbMn_2O_5$ were obtained through a two-step synthesis. These $TbMn_2O_5$ nanowires have high crystallinity and high aspect ration. They can be as long as tens of micrometers with a minimum diameter of about 20 nm. Analysis based on HRTEM demonstrate their grow direction is along (001). Their growth mechanism was discussed. In the case of magnetism, $TbMn_2O_5$ nanowires turn out to be paramagnetic at high temperature and weak ferromagnetic at low temperature. ZFC and FC curves separated below about 45 K and a transition peak at 4 K of ZFC is observed. Magnetic hysteresis loop of $TbMn_2O_5$ measured at 5 K shows a coercivity of 35 Oe. Measurements of dielectric constant ε and dielectric loss tan δ reflect a sustainable upward rising (especially above 200 K) and this tendency increased with the drop of frequencies. Under lower frequencies the peak positions of dielectric loss shifted towards higher temperature.

Introduction

Multiferroic materials such as $TbMn_2O_5$,[1,2] $BiFeO_3$,[3,4] $TbMnO_3$,[5,6] $YMnO_3$,[7] $BiMnO_3$[8] et al.[9-12] have attracted widespread attentions during the past decade. Possessing more than one of ferromagnetic, ferroelectric and ferroelastic properties simultaneously, they have great potentials in multifunctional devices,[4,13-15] for example four-state memories, in which both magnetization and polarization could independently encode in a single multiferroic bit. Or magnetism and ferroelectricity could be coupled, which enables date to be written electrically and read magnetically. Magnetoelectric coupling may also make it possible of varieties of magnetoelectric devices like electric field controlled electromagnetic resonances and magnetic field controlled piezoelectric sensors and so on.[16]

Multiferroic manganite materials such as $TbMnO_3$ and $TbMn_2O_5$ have attracted extensive interests since 2003 when Kimura and Tokura et al. reported the discovery of ferroelectricity in a pervoskite manganite, $TbMnO_3$,[5] where the spontaneous polarization could be switched by applied magnetic field. Then in 2004, Hur et al. reported a profound interplay between electrical polarization and the applied magnetic field in $TbMn_2O_5$ as well.[1] That means they possess strong magnetoelectric coupling and therefore became new candidate materials for magnetoelectric medias.

However because of their low intensity of polarization and the demand of specific conditions, low temperature for instance,[10,17] there is still a long way to go before they could make a real contribution to the data storage industry. Thus significant developments of multiferroic materials are required, such as nanoscale materials. In fact most researches about multiferroic materials are based on bulks or films, so there are still lots to be done in nanoscale.[18-22] When it comes to nanoscale, materials are expected to display enhanced properties[23-24], or even completely new fascinating properties compared with their bulk forms.[25-30] And as is known that magnetic and electrical properties of multiferroic materials, especially nano-materials are highly depend on their crystal structures and morphologies, such as sizes, dimensions and defects.[31-35] So it is of great significance to synthesis nanoparticles in a controlled manner. Therefor researches about multiferroic materials in nanoscale will certainly promote their extensive applications in the future.

In this letter, we described single crystal bunched $TbMn_2O_5$ nanowire clusters which were obtained through high temperature annealing after solution synthesis in acid. These $TbMn_2O_5$ nanowires have high aspect rations as they can be as long as tens of micrometers with a minimum diameter of about 20 nanometers.

Experiment

To prepare $TbMn_2O_5$ nanowire, 1.0 mmol Tb_4O_7 and 8.0 mmol $MnCl{\bullet}4H_2O$ were dissolved in distilled water and excess HCl solution were added in. Different from traditional methods[31,36,37] the reaction proceeded throughout in acid solution and no alkali was addied in. After 24 h's stirring in atmospheric pressure under 70 °C, the puce solution turn to colorless and transparent. Then quit stirring and maintain temperature at 70 °C to evaporate redundant HCl and Water until the formation of pink crystals. After grinding to fine powders, they were transferred into a tube furnace and heated at 800 °C for 5 h in air under atmospheric pressure, then $TbMn_2O_5$ nanowires came to its formation.

Key Laboratory of Micro-nano Measurement-Manipulation and Physics (Ministry of Education), Department of Physics, Beihang University, Beijing 100191, China

* To whom correspondence should be addressed.

E-mail: cuiym@buaa.edu.cn

Results and discussion

Their morphologies and microstructures investigated by scanning electron microscopy (SEM) are shown in Fig. 1. We can see that, these bunched nanowires formed clusters covering the entire surface of our samples. Every cluster consists of hundreds of nanowires that have a length of tens of micrometers while their diameters vary from 20 nm to 200 nm with an average value of about 50 nm. More interestingly, fancy structured rectangular nanotubes were obtained in some of our samples reacted in alkaline solutions (add defined amount of KOH into the colorless and transparent solutions that have already reacted for 24 h) and decrease annealing time to 2 h at the last step. Their thin tube walls are quite smooth and obviously vertical to each other. The cross section dimension is about 1 μm × 1 μm.

In fact, other various novel nanoparticles were also discovered with different morphologies, like hexagram (Fig. 2a), regular octahedron (Fig. 2b), acicular (Fig. 2c), hexagon piece (Fig. 2d), nanorods (Fig. 2e) and rectangle piece (Fig. 2f). They are prepared in the same method as $TbMn_2O_5$ nanowire clusters, but experimental conditions are different, such as different annealing temperature, reaction time or reactant ratio. However, to prepare them in a controlled manner is still under research. So the measurements of structures and properties that will be discussed later in this paper are all about $TbMn_2O_5$ nanowires.

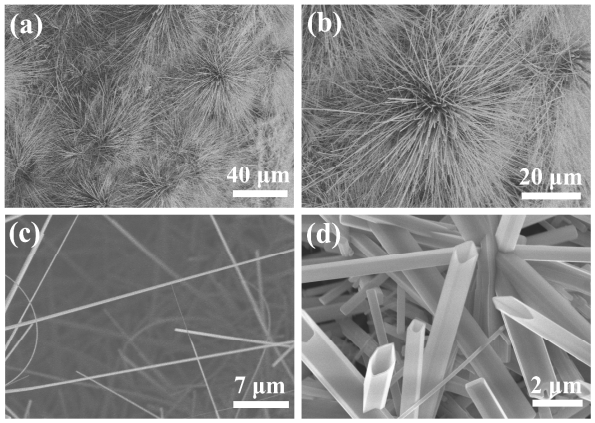

Fig. 1 (a)-(c) SEM images of $TbMn_2O_5$ nanowire clusters. (d) SEM images of rectangular nanotubes.

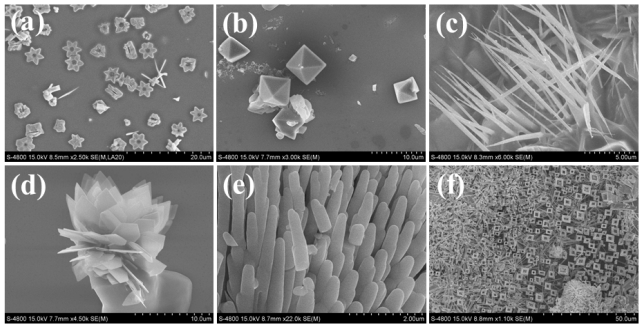

Fig. 2 SEM images of nanoparticles with different morphologies: (a) hexagram, (b) regular octahedron, (c)acicular, (d)hexagon piece, (e)nanorods, (f) rectangle piece.

The crystallinity and composition of $TbMn_2O_5$ nanowires were examined by X-ray diffraction (XRD) (Fig. 3). All diffraction peaks were perfectly indexed by an orthorhombic phase with space group Pbam (No. 55). The lattice parameters are a=7.343, b=8.572, c=5.647.

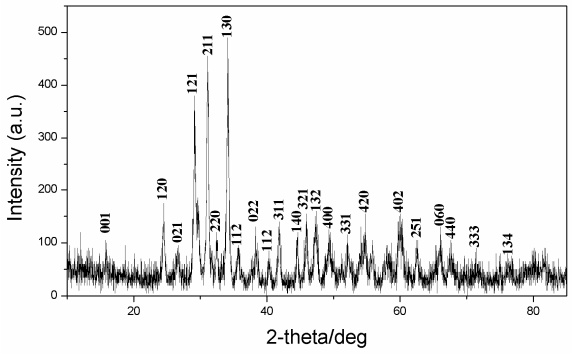

Fig. 3 XRD patterns of $TbMn_2O_5$ nanowires.

The reaction process can be described as two steps. Firstly, Tb_4O_7 react with HCl and generate a mixed solution contains $TbCl_3$ and $TbCl_4$. After the evaporation of redundant HCl and water, they were transferred into a tube furnace. When anneal in 800 ^oC for 5 h, $TbCl_3$, $TbCl_4$ and $MnCl_2{\cdot}4H_2O$ were oxidized to $TbMn_2O_5$ crystals by O_2 in the air. The formation of $TbMn_2O_5$ can be written as follows:

$$Tb_4O_7 + 14HCl \rightarrow 2TbCl_3 + 2TbCl_4 + 7H_2O \quad (1)$$

$$4TbCl_3 + 4TbCl_4 + 16MnCl_2{\cdot}4H_2O + 5O_2 \rightarrow 8TbMn_2O_5 + 60HCl\uparrow + 34H_2O\uparrow \quad (2)$$

To determine crystal orientation and grow direction of $TbMn_2O_5$ nanowires, transmission electron microscopy and high-resolution TEM were used (Fig. 4). The HRTEM images shows distinct lattice fringe images with interplanar distances of 0.552 nm (Fig. 4c) and 0.359 nm (Fig. 4d) which are correspond to (001) and (200) planes respectively. Take the directions of lattice fringes into consideration (lattice fringes in Fig. 4c are vertical to growth direction and in Fig. 4d parallel to growth direction), we can draw the conclusion that these single crystal $TbMn_2O_5$ nanowires grow along [001] direction, which should correspond to a lower energy and a more stable state.[31]

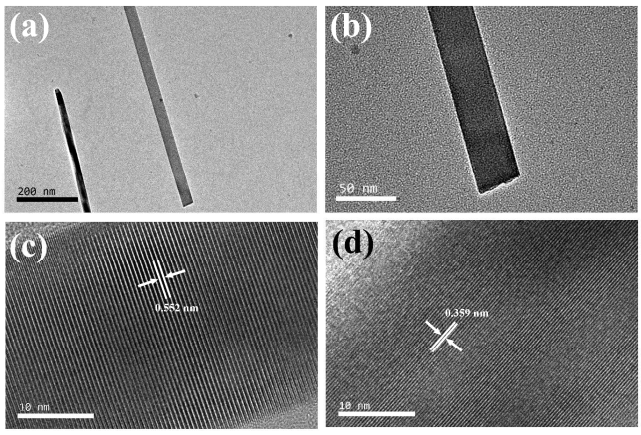

Fig. 4 (a) (b) are TEM images of $TbMn_2O_5$ nanowires; (c) HRTEM image of a single $TbMn_2O_5$ nanowire with lattice fringes vertical to growth

direction; (d) HRTEM image of a single $TbMn_2O_5$ nanowire whose lattice fringes are parallel to growth direction.

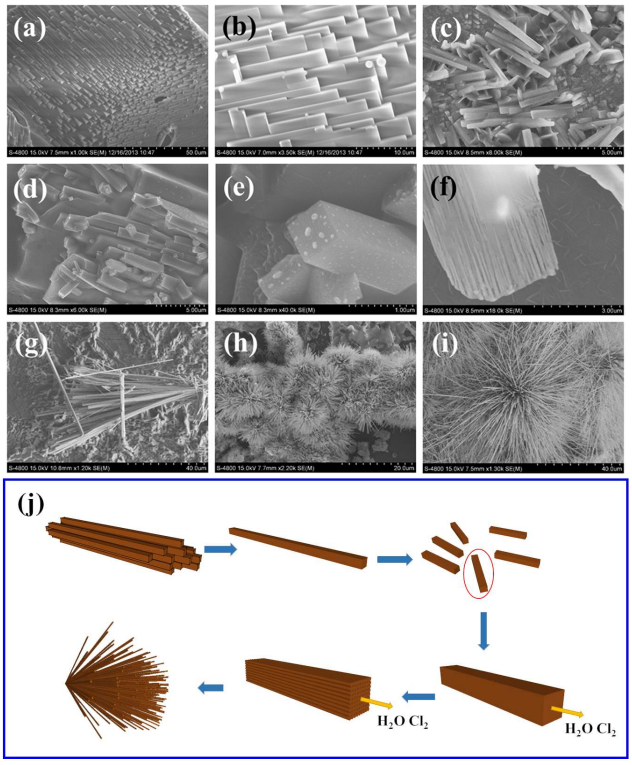

Fig. 5 The formation process of $TbMn_2O_5$ nanowire clusters. (a) (b) long cuboid crystals stacked together forming step-like structures. (c)-(e) long cuboids broke into several shorter parts. (f) every cuboid broke into a large number of thin and straight nanowires with the generation of H_2O and HCl. (g) these nanowires separated from each other on top while kept together on bottom. (h) (i) with the increase of annealing time, more and more nanorods and nanowires broke into thinner nanowires and $TbMn_2O_5$ nanowire clusters came into being. (j) Schematic growth mechanism of $TbMn_2O_5$ nanowire clusters.

Based on the SEM images of samples with different annealing time, we put forward one possible growth mechanism of $TbMn_2O_5$ nanowire clusters which is shown in Fig. 5. At the beginning of high temperature annealing, reactants crystallized to long cuboid and stacked together forming step-like structures. Then they broke into several shorter parts with the contribution of high temperature. As reaction went on, gases such as H_2O and HCl generated and were exhausted from these cuboids. These gases not only broke existing chemical bonds but also drove different parts of crystal separated from each other and there formed straight nanorods or nanowires. The top of them were separated from each other while the bottom are still together. With the increase of annealing time, more and more nanorods and nanowires broke into thinner nanowires. So finally $TbMn_2O_5$ nanowire clusters came into being.

The temperature dependent magnetizations were measured by zero-field-cooled (ZFC) and field-cooled (FC) conditions in a magnetic field of 100 Oe (Fig. 6a). The magnetization curves show a sharp increase in magnetization with decreasing temperature under 50 K. This is regarded as ferromagnetic-like. In particular, transition peaks at about 5 K and 17 K are observed in Fig. 6b, which may be related to the ordering temperature of Tb ion spins and lock-in transition temperature of $TbMn_2O_5$ respectively. These two temperatures in another homologous bulk manganite $TbMnO_3$ are 7 K and 27 K[5] while in $TbMnO_3$ films they are 10 K and 32 K.[6] ZFC and FC curves separated below 45 K (inset of Fig. 6a).

Above Néel temperature (about 50 K), reciprocal of magnetic susceptibility χ shows good linearly dependent to temperature, that means magnetic susceptibility obeys Curie-Weiss law well (χ=C/(T-θ)). Analysis indicate Curie constant C is 0.0378 emuK/gOe and Curie temperature θ is -24.15 K for field-cooled (FC) and C=0.0376 emuK/gOe, θ = -22.48 K for zero-field-cooled (ZFC) (Fig. 6c).

Magnetic hysteresis loops of $TbMn_2O_5$ measured at 5 K and 100 K are shown in Fig. 6d. They are liner-type at 100 K and S-type at 5 K (with a coercivity of 35 Oe) (inset of Fig. 6d). These signify $TbMn_2O_5$ to be paramagnetic at high temperature and weak ferromagnetic at low temperature.

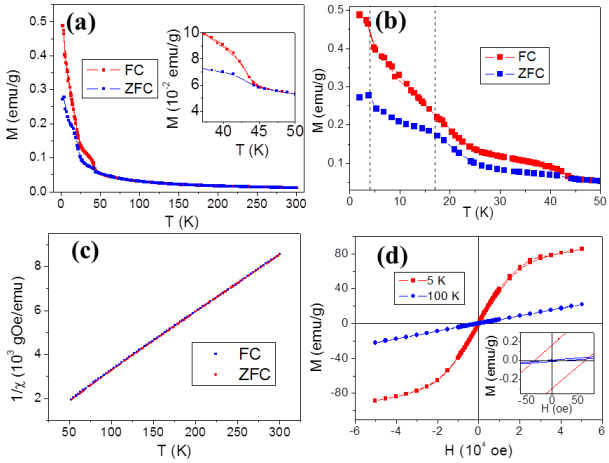

Fig. 6 (a) Temperature dependent of field-cooled (FC) and zero-field-cooled (ZFC) magnetization from 3 K to 300 K measured in a field of 100 Oe. The inset shows the separation between FC and ZFC curves. (b) The enlarged temperature dependent of FC and ZFC magnetization from 3 K to 50 K measured in a field of 100 Oe. (c) Liner fit of 1/χ with temperature. (d) Field-dependent magnetization at 5 K and 100 K. The inset is the enlarged M-H shows coercivity.

Finally, we show in Fig. 7 the temperature dependent of dielectric constant ε and dielectric loss tan δ measured under different frequencies, 100 Hz, 120 Hz, 1 kHz, 10 kHz, 20 kHz, 50 kHz and 100 kHz.

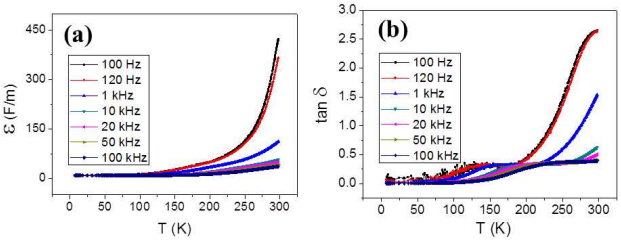

Fig. 7 (a) and (b) are temperature dependent of dielectric constant ε and dielectric loss tan δ respectively, measured at 100 Hz, 120 Hz, 1 kHz, 10 kHz, 20 kHz, 50 kHz and 100 kHz.

The curves of dielectric constant ε are smooth without any significant peaks. The behavior reflects a sustainable upward rising and this tendency increased with the drop of frequency. As for the dielectric losses, peaks around 150 K are observed and the peak positions shifted towards higher temperature when frequencies are lower. Above 200 K both dielectric constants and dielectric losses of low frequencies, such as 100 Hz and 150 Hz, became quite fast growing compared with higher frequencies.

Conclusions

Single crystal bunched $TbMn_2O_5$ nanowire clusters with high degree of crystallinity were obtained through a two-steps synthesis (solution reaction and followed by high temperature annealing). During high temperature annealing, they turn from step-like structures to nanowire clusters with generation of H_2O and HCl. These $TbMn_2O_5$ nanowires have high aspect rations that they can be as long as tens of micrometers with a minimum diameter of about 20 nm. Analysis based on HRTEM demonstrate their grow direction to be along (001). In the case of magnetism, $TbMn_2O_5$ nanowires turn out to be paramagnetic at high temperature and weak ferromagnetic at low temperature. ZFC and FC curves separated below about 45 K and a transition peak at 4 K of ZFC is also observed. Magnetic hysteresis loop of $TbMn_2O_5$ measured at 5 K shows a coercivity of 35 Oe. Measurements of dielectric constant ε and dielectric loss tan δ reflect a sustainable upward rising (especially above 200 K) and this tendency increased with the drop of frequency. Under lower frequencies the peak positions of dielectric loss shifted towards higher temperatures.

Acknowledgements

We acknowledge the financial support from the National Natural Science Foundation of China (No. 10975013).

Notes and references

[1] N. Hur, S. Park, P. A. Sharma, J. S. Ahn, S. Guha and S. W. Cheong, *Nature*, 2004, **429**, 392-395.
[2] L. C. Chapon, G. R. Blake, M. J. Gutmann, S. Park, N. Hur, P. G. Radaelli and S. W. Cheong, *Phys. Rev. Lett.,* 2004, **93**, 177402.
[3] J. Wang, J. B. Neaton, H. Zheng. V. Nagarajan, S. B. Ogale, B. Liu, D. Viehland, V. Vaithyanathan, D. G. Schlom, U. V. Waghmare, N. A. Spaldin, K. M. Rabe, M. Wutting and R. Ramesh, *Science*, 2003, **299**, 1719-1722.
[4] G. Catalan and J. F. Scott, *Adv. Mater.,* 2009, **21**, 2463-2485.
[5] T. Kimura, T. Goto, H. Shintani, K. Lshizaka, T. Arima and Y. Tokura, *Nature*, 2003, **426**, 55-58.
[6] Y. M. Cui, Y. F. Tian, A. X. Shan, C. P. Chen and R. M. Wang, *Appl. Phys. Lett.,* 2012, **101**, 122406.
[7] M. Fiebig, T. Lottermoser, D. Frohlich, A. V. Goltsev and R. V. Pisarev, *Nature,* 2002, **419**, 818-820.
[8] T. Kimura, S. Kawamoto, I. yamada, M. Azuma, M. Takano and Y. Tokura, *Phys. Rev. B*, 2003, **67**, 180401.
[9] W. Eerenstein, N. D. Mathur and J. F. Scott, *Nature*, 2006, **442**, 759-765.
[10] N. A. Hill, *J. Phys. Chem. B,* 2000, **104**, 6694-6709.
[11] R. Ramesh, N. A. Spaldin, *Nat. Mater.,* 2007, **6**, 21-29.
[12] C. W. Nan, M. I. Bichurin, S. X. Dong, D. Viehland and G. Srinivasan, *J. Appl. Phys*., 2008, **103**, 031101.
[13] X. F. Li, J. D. Budai, F. Liu, J. Y. Howe, J. H. Zhang, X. J. Wang, Z. J. Gu, C. J. Sun, R. S. Meltzer and Z. W. Pan, *Light-Sci. Appl.,* 2013, **2**, e50.
[14] D. N. Nath, Z. C. Yang, C. Y. Li, P. S. Park, Y. R. Wu and S. Rajan, *Appl. Phys. Lett.,* 2013, **103**, 022102.
[15] S. W. Cheong and M. Mostovoy, *Nat. Mater.* 2007, **6**, 13-20.
[16] J. F. Scott, *J. Mate. Chem.,* 2012, **22**, 4567-4574.
[17] J. Ma, J. M. Hu, Z. Li and C. W. Nan, *Adv. Mater.,* 2011, **23**, 1062-1087.
[18] P. M. Rorvik, T. Grande and M. A. Einarsrud, *Adv. Mater.,* 2011, **23**, 4007-4034.
[19] N. Jeon, D. rout, I. W. Kim and S. J. L. Kang, *Appl. Phys. Lett.,* 2011, **98**, 072901.
[20] B. Liu, B. B. Hu and Z. L. Du, *Chem. Commun.,* 2011, **47**, 8166-8168.
[21] N. Choudhury, L. Walizer, S. Lisenkov and L. Bellaiche, *Nature*, 2011, **470**, 513-517.
[22] W. Prellier, M. P. Singh and P. Murugavel, *J. Phys-Condens. Mat.,* 2005, **17**, 803-832.
[23] A. Lundskog, C. W. Hsu, K. F. Karlsson, S. Amloy, D. Nilsson, U. Forsberg, P. O. Holtz and E. Janzen, *Light-Sci Appl.,* 2014, **3**, e139.
[24] G. Z. Xing, Y. Wang, J. I. Wong, Y. M. Shi, Z. X. Huang, S. Li and H. Y. Yang, *Appl. Phys. Lett.,* 2014, **105**, 143905.
[25] A. Sundaresan and C. N. R. Rao, *Nano Today,* 2009, **4**, 96-106.
[26] I. Levin, J. H. Li, J. Slutsker and A. L. Roytburd, *Adv. Mater.,* 2006, **18**, 2044-2047.
[27] J. Chen, X. R. Xing, A. Waston, W. Wang, R. B. Yu, J. X. Deng, L. Yan, C. Sun and X. B. Chen, *Chem. Mater*., 2007, **19**, 3598-3600.
[28] S. M. Selbach, T. Tybell, M. A. Einarsrud and T. Grande, *Chem. Mater.*, 2007, **19**, 6478-6484.
[29] R. Mazumder, P. S. Devi, D. Bhattacharya, P. Choudhury, A. Sen and M. Raja, *Appl. Phys. Lett.,* 2007, **91**, 062510.
[30] C. W. Nan, G. Liu, Y. H. Lin and H. D. Chen, *Phys, Rev. Lett.,* 2005, 94, 197203.
[31] J. T. Han, Y. H. Huang, W. Huang and J. B. Goodenough, *J. Am. Chem. Soc.*, 2006, **128**, 14454-14455.
[32] P. K. Zhang and Y. M. Cui, *CrystEngComm.*, 2013, **15**, 9963-9967.
[33] Y. M. Cui, W. Liu and R. M. Wang, *Phys. Chem. Chem. Phys.,* 2013, **15**, 6804-6808.
[34] T. J. Park, G. C. Papaefthymiou, A. J. Viescas, A. R. Moodenbaugh and S. S. Wong, *Nano Lett.,* 2007, **7**, 766-772.
[35] S. Zhong, S. B. Duan and Y. M. Cui, *RSC Adv.,* 2014, **4**, 40924-40929.
[36] X. X. An, J. X. Deng, J. Chen and X. R. Xing, *Mater. Res. Bull.*, 2013, **48**, 4984-4988.
[37] S. M. Khule and S. A. Acharya, *J. Exp. Nanosci.*, 2013, **8**, 288-294.

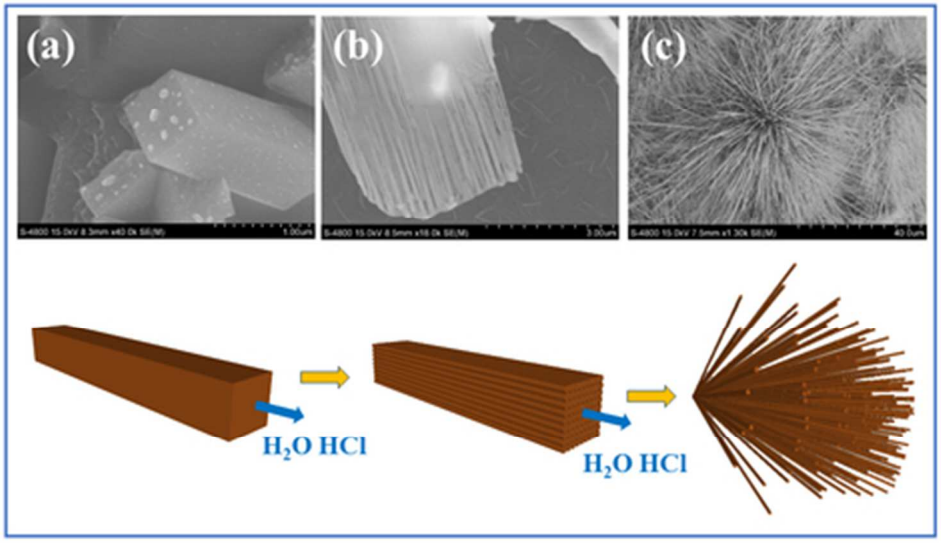

Colour graphic
39x23mm (300 x 300 DPI)

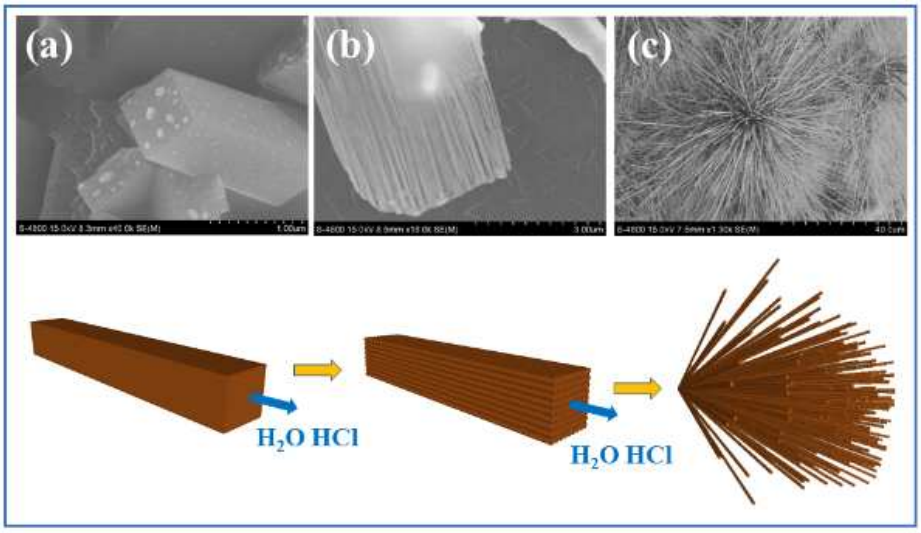

Single crystal nanowire clusters of multiferroic material $TbMn_2O_5$ were obtained through a simple two-step method.